# Exploitation of nanoparticle-protein interactions for early disease detection

Massimiliano Papi, Valentina Palmieri (iD), Sara Palchetti, Daniela Pozzi, Luca Digiacomo, Elia Guadagno, Marialaura del Basso De Caro, Marina Di Domenico, Serena Ricci, Roberto Pani, Morteza Mahmoudi, Angelina Di Carlo, and Giulio Caracciolo

View Online    Export Citation    CrossMark

# Exploitation of nanoparticle-protein interactions for early disease detection

Massimiliano Papi,[1,2,a)] Valentina Palmieri,[1,2,a)] (ID) Sara Palchetti,[3] Daniela Pozzi,[3] Luca Digiacomo,[3] Elia Guadagno,[4] Marialaura del Basso De Caro,[4] Marina Di Domenico,[5,6] Serena Ricci,[7] Roberto Pani,[7] Morteza Mahmoudi,[8] Angelina Di Carlo,[7] and Giulio Caracciolo[3,b)]

## AFFILIATIONS

[1] Fondazione Policlinico A. Gemelli IRCCS, Roma, Italy
[2] Università Cattolica Sacro Cuore. Istituto di Fisica, Largo Francesco Vito 1, 00168 Roma, Italy
[3] Department of Molecular Medicine, Sapienza University of Rome, Viale Regina Elena 291, 00161 Rome, Italy
[4] Department of Advanced Biomedical Sciences, Pathology Section, University of Naples "Federico II," Via S. Pansini 5, 80131 Naples, Italy
[5] Department of Precision Medicine, Università degli Studi della Campania "Luigi Vanvitelli," Via L. De Crecchio, 7, 80138 Naples, Italy
[6] Department of Biology, College of Science and Technology, Temple University, 1803 N Broad St #400 Philadelphia, Pennsylvania 19122, USA
[7] Department of Medico-Surgical Sciences and Biotechnologies, "Sapienza" University of Rome, Corso della Repubblica 79, Latina 04100, Italy
[8] Center for Nanomedicine and Department of Anesthesiology, Brigham and Women's Hospital, Harvard Medical School, Boston, Massachusetts 02115, USA

[a)] **Contributions:** M. Papi and V. Palmieri contributed equally to this work.
[b)] **Author to whom correspondence should be addressed:** giulio.caracciolo@uniroma1.it

## ABSTRACT

The main diagnostic tools for primary and metastatic central nervous system (CNS) tumors are the anamnestic neurological examination and the imaging tests, which are expensive and lack specificity. In recent years, the shell of macromolecules which forms on nanoparticles (NPs) when they are exposed to human blood, also known as hard corona (HC), became a powerful tool in diagnostics. Indeed, HC can act as a "nano-concentrator" of serum proteins and can detect minor changes in the protein concentration at the very early stages of disease development. In this paper, we characterized lipid NP HC formed in blood samples from patients affected by meningeal tumors. We found that the HCs of meningeal tumor patients could be discriminated from those of healthy subjects. Our results show that emerging HC-based technologies will pave the way for early diagnosis of CNS cancer.

*Published under license by AIP Publishing.* https://doi.org/10.1063/1.5098081

Tumors of the central nervous system (CNS) represent one of the most common causes of cancer death and account for about 1.3% of all malignant cancer, with an incidence of 7 per 100 000 persons worldwide.[1,2] CNS tumors consist of a heterogeneous group of neoplasms, including different variants of primary brain tumors (glial or nonglial, benign, or malignant) and metastatic neoplasms.[3] Metastatic brain tumors include malignant tumors that arise elsewhere in the body (such as the breast or lungs) and migrate to the brain, usually through the bloodstream. The number of primary and metastatic brain tumors is steadily rising, whereas the mortality rate for most tumor types has remained essentially unchanged. In particular, patients with high-grade glioma usually have the worst prognosis with a median survival of 12 months even after surgical resection, radiation therapy, and chemotherapy.[4] Actually, the main diagnostic tools for both primary and metastatic CNS tumors are the anamnestic neurological examination and the imaging tests, such as conventional magnetic resonance and computerized tomography scan.[2] Advanced imaging techniques improve the neuro-radiological diagnostic accuracy; however, they are expensive and lack specificity, and thus, there is a pressing need of noninvasive methods to diagnose carcinoma of the CNS as well as for their management. Currently, except for rare germ cell tumors, there is no method to prospectively detect brain
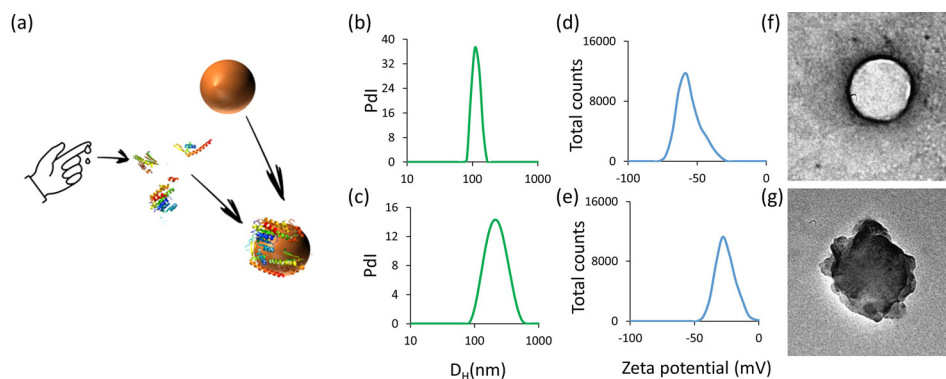
**FIG. 1.** (a) Schematic illustration of the protocol used for HC formation. The probability density function weight with the intensity (PdI) vs liposome's (b) and HC-liposome's hydrodynamic diameter ($D_H$) (c). Zeta potential distributions of liposomes before (d) and after (e) incubation with HP. Representative TEM images of liposomes (f) and HC-liposomes (g).

tumor until they have progressed to the symptomatic stage. Thus, detection, definition, and validation of biomarkers for diagnosis, prognosis, disease monitoring, as well as therapeutic efficacy and tumor progression are recognized as tough challenges in oncologic research. Recent advances in nanotechnology have brought many innovative approaches to cancer diagnosis. Due to the peculiar properties that arise when a material is reduced to the nanoscale, nanoparticles (NPs) are being utilized in almost limitless applications.[5] When dispersed in a biological fluid, the NP surface interacts with medium components. The result is the development of a dynamic interface on the NP surface, the so-called "bio-nano interface," composed of biomolecules such as proteins, sugars, and lipids. This biomolecular shell is dynamic by nature, and given the protein enrichment, it is usually referred to as the protein corona (PC).[6] PC is made of the "hard" corona (HC) and the "soft" corona (SC). HC is made of proteins strongly adsorbed to the surface and is the interface "seen" and processed by living systems.[7] The formation and composition of HC depend on several factors:[8,9] (i) surface properties of NPs (i.e., size, shape, curvature, surface chemistry, and surface charge); (ii) characteristics of biological media, including the protein concentration, protein source, and temperature; and (iii) incubation time.[10] Since the protein pattern in cancer patients' blood differs from that of healthy donors, the molecular composition of the HC formed around NPs could change between cancer and non-cancer patients. Therefore, HC can act as a nanoconcentrator[11] of serum proteins with affinity for the NP surface. Characterization of HC could therefore allow detection of small changes in the protein concentration at the very early stages of disease development when alterations in the circulating levels of proteins are undetectable by blood tests. In this work, we explored the feasibility of developing a technology for CNS tumor HC detection, based on a method recently reported for pancreatic cancer detection.[12] To this end, we employed a liposomal formulation made of 1,2-dioleoyl-sn-glycero-3-phospho-(1'-rac-glycerol) (DOPG).[13] Blood samples from 25 meningeal tumors and 20 healthy subjects were analyzed. Patients were excluded if they: (i) had other concomitant illnesses; (ii) had evidence of recent history of intracranial hemorrhage; and (iii) did not have a definitive diagnosis at the end of diagnostic work-up. In all meningiomas, Ki-67 protein and progesterone receptor (PR) staining was performed. Diagnosis of tumors was made by usual clinical criteria and confirmed postoperatively by histopathological findings according to the latest WHO classification.[3] 10 healthy volunteers with no concomitant illnesses, infections, gastrointestinal disease, hepatic disease, or renal disease nor

tumors or immunological disease were used as controls. The values of basic laboratory parameters of these participants were within the reference limits. Peripheral venous blood samples were collected preoperatively. For each sample, determination of the protein concentration was performed using the method of Bradford.[9] Human plasma (HP) preparation was performed according to the methods already described. Liposomes were incubated with HP (1:1 v/v) at 37 °C for 1 h according to previous investigations.[14] After incubation, liposome–protein complexes were isolated by 3 consecutive centrifugations for 15 min at 14 000 rpm and resuspension in phosphate buffered saline (PBS) to remove unbound proteins and to obtain the hard corona (HC). The HC-coated liposomes were analyzed on a gradient polyacrylamide gel (4%–20% Criterion Tris-Glycine eXtended (TGX) precast gels, Bio-Rad). Proteins were stained with highly sensitive silver-ammonia solution. Pictures of gels were captured using a KODAK Digital DC120. Densitometry analysis was performed using ImageJ.[15] Measurements of the size and surface charge were performed using a Zetasizer Nano ZS90 (Malvern, UK) as reported elsewhere.[16] For Electron Microscopy, samples were stained with 2% uranyl acetate and imaged using a TEM SUPRA 25 (Zeiss, Germany). Nanoliquid chromatography tandem mass spectrometry (nanoLC/MS-MS) was performed using a Dionex Ultimate 3000 (Sunnyvale,
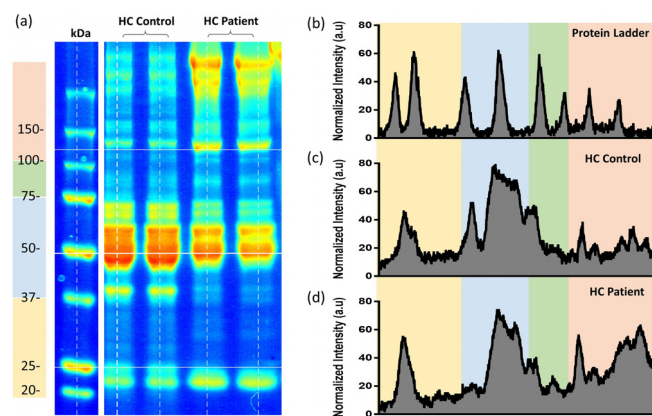


**FIG. 2.** (a) Representative SDS/PAGE with a ladder and a duplicated HC of the control and patient sample. The four regions used for integral area analysis are highlighted. Intensity profiles of ladder (b), representative HC of a control (c), and representative HC of a patient are shown. Areas for the integral calculation have been highlighted.

CA, USA) nanoLC system connected to a hybrid mass spectrometer LTQ Orbitrap XL (Thermo Fisher Scientific Bremen, Germany), furnished with a nanoelectrospray ion source. Sample preparation and data analysis have been performed following a protocol reported elsewhere.[17]

As illustrated in Fig. 1(a), bare liposomes have been incubated with human plasma (HP) to allow the formation of HC. Dynamic light scattering (DLS) has been used to measure the size of liposomes before and after incubation [Figs. 1(b) and 1(c), respectively]. Size distributions are unimodal and centered at $D_H = 150 \pm 11$ nm in the case of bare liposomes and $D_H = 202 \pm 12$ nm for HC-liposomes. Zeta potential distributions are also reported and centered at $\zeta = -59 \pm 5$ mV in the case of bare liposomes [Fig. 1(d)] and $\zeta = -31 \pm 3$ mV for HC-liposomes [Fig. 1(e)]. The increase in the size and variation of Zeta potential demonstrate the formation of the HC. TEM images confirm DLS data since while bare liposomes have a smooth surface
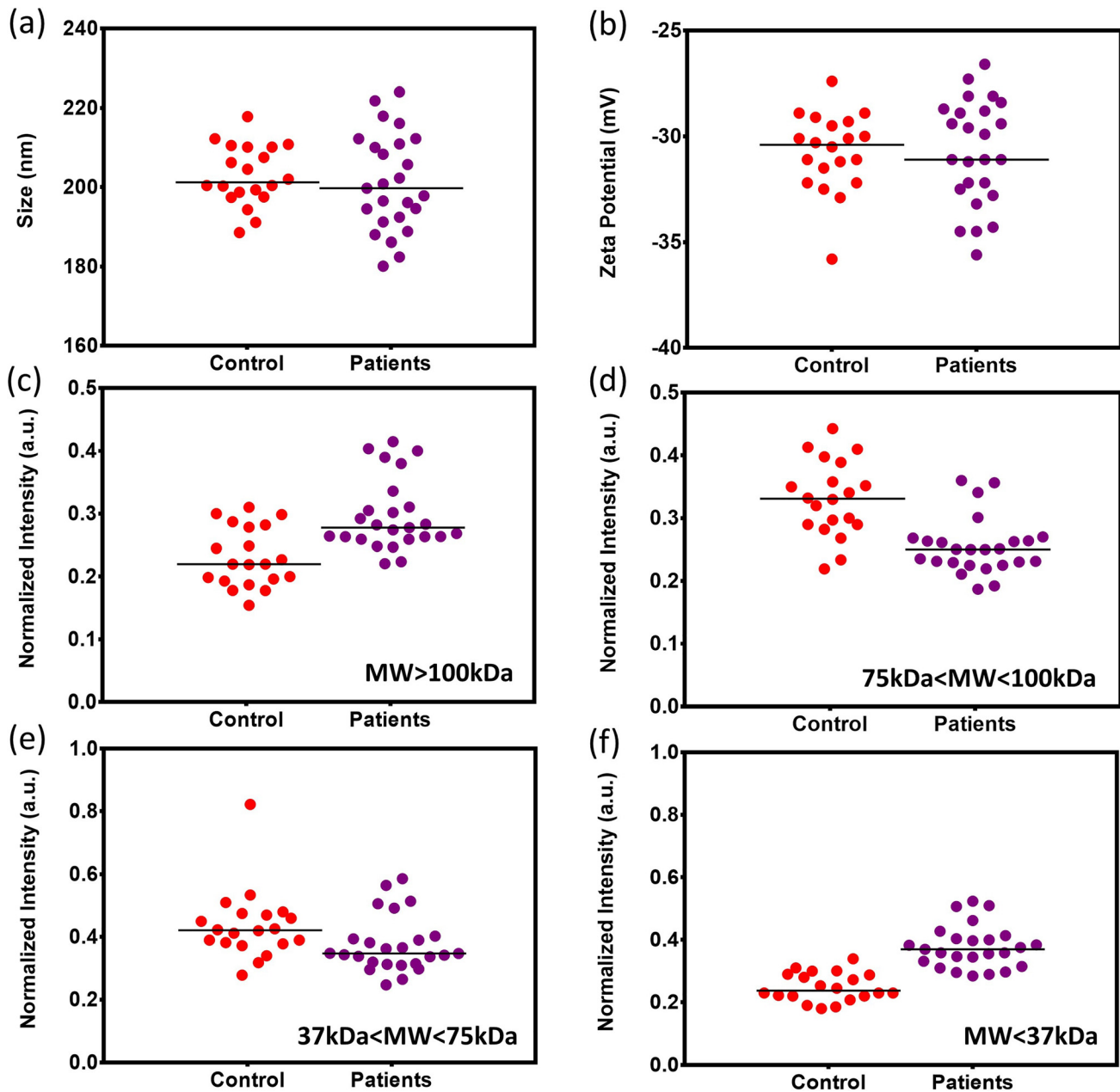


**FIG. 3.** Comparison of control's and patient sample's HC: diameter (a) and Zeta potential of HC-liposomes (b); integral areas of intensity profiles for MW > 100 kDa (c), 75 kDa < MW < 100 kDa (d), 37 kDa < MW < 75 kDa (e), and MW < 37 kDa (f). Average values are reported with a black bold line in each graph.

[Fig. 1(f)], a dense negatively stained area (i.e., the HC) surrounds liposomes after incubation with HP [Fig. 1(g)].

The HCs were detached from the liposomes and analyzed by 1D sodium dodecyl sulfate polyacrylamide gel electrophoresis (SDS/PAGE). In Fig. 2(a), a representative SDS/PAGE is reported with ladder in the first lane and a HC sample duplicate in the second and third lanes. Intensity profiles have been calculated along vertical dashed lines, and the ladder intensity profile in Fig. 2(b) is compared with a patient intensity profile in Fig. 2(c). The mass distribution of HC in our samples is characterized by three major protein bands located at $\approx 150$ kDa, 50 kDa, and 25 kDa with protein concentrated in the central region of the SDS PAGE. For this reason, we divided average lane intensity profiles into 4 regions with similar protein abundance (i) $MW < 37$ kDa; (ii) $37$ kDa $< MW < 75$ kDa; (iii) $75$ kDa $< MW < 100$ kDa; and (iv) $MW > 100$ kDa.

In Fig. 3, the values of size, charges, and normalized intensity areas obtained from SDS PAGE analysis are displayed. While the average values of the size and Zeta potential of HC-liposomes do not display statistically significant differences between healthy and cancer patients, the normalized intensity shows subtle differences. The average values of intensity are higher for controls in the regions between 75 kDa–100 kDa and 37 kDa–75 kDa. In contrast, in the other SDS/PAGE regions, the average values are higher for cancer patients. Despite these evidences, distributions of normalized intensities are overlapped and therefore not feasible for cancer detection.

For this reason, we applied (Principal component analysis) PCA to our results.[18] PCA was performed using the four integral areas, size, and zeta potential as variables, and Linear Discriminant Analysis (LDA) on principal components has been used to divide healthy and cancer patients in the PC1 and PC2 plane.[19] The results in Fig. 4 demonstrate that PCA-LDA is capable of discriminating the two groups as shown by separation of the PC centroids [Fig. 4(b)]. Variances explained by PC1 and PC2 are 38.2% and 31.6%, respectively. These two PCs are strongly determined by the protein mass distribution, whereas PC3 and PC4 take in account mainly the physical parameters (size and zeta potential) with a variance of 14% and 12%, respectively.

In Fig. 3 is clearly visible how the largest differences in protein corona intensity rely on the molecular weight range between 75 kDa and 100 kDa [Fig. 3(d)]. To verify if this difference is merely caused by a lower protein concentration or by a different pattern of adsorbed proteins, we analyzed by mass spectroscopy this specific range of gel bands. The results are shown in Fig. 4(c). In the color map, proteins are grouped into proteins visible only in healthy patients' corona [Unique (H)], proteins more abundant in the healthy group (H > C), proteins more abundant in the cancer group (C > H), and specific proteins of cancer patients' corona [Unique (C)]. 6 proteins are unique in cancer patients' protein corona: Lactotransferrin, Integrin beta-2, Myeloperoxidase, Phosphatidylinositol-glycan-specific phospholipase D, Polymeric immunoglobulin receptor, and Desmocollin-1. Among these proteins, Desmocollin-1 is of particular interest for its involvement in transition from normal to malignant tissue and has been proposed as a biomarker for intracranial tumors in histochemistry diagnostics.[20] Also, Lactotransferrin was reported as a possible biomarker for brain tumor in a previous study.[21] These evidences demonstrate that the different gel band intensity are generated by a specific pattern of proteins, already considered as brain tumor biomarkers, which are absorbed in the biomolecular corona of cancer patients.
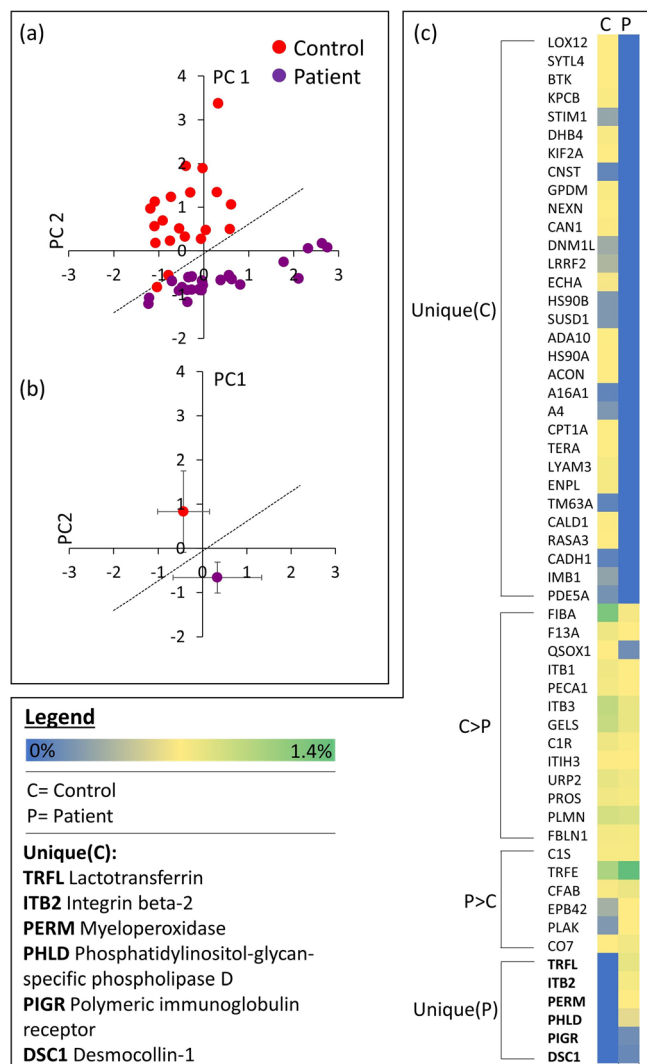


**FIG. 4.** (a) PC1 and PC2 calculated by PCA analysis of healthy and cancer patients. (b) Centroids of the distributions. The line separates the controls from the cancer patient group, according to the results of LDA. (c) Proteins detected in the healthy (H) and cancer patients' (C) plasma protein corona in the range of 75 kDa < Mw < 100 kDa. Colors express the Relative Protein Abundance (%RPA) from 0% (blue) to 1.4% (green). Unique Cancer group proteins [Unique (C)] are listed. Proteins with higher abundance in healthy and cancer patients are also reported as H > C and C > H, respectively.

Since nowadays there is no method to detect brain tumor before its symptomatic stage, the development of a sensitive and specific biomarker could open huge medical opportunities in terms of treatment and outcomes. Exploiting the nanobio-interactions between NP and blood samples, we investigated the feasibility of developing a diagnostic technology for meningeal tumor detection. Our results highlight how small differences in the plasma composition, not visible by conventional blood testing, between healthy volunteers and patients suffering from meningeal tumor are amplified in the nanoparticle protein corona composition. It is important to point out that these differences

can be quantitatively appreciated using a relatively inexpensive and fast technique such as 1D gel-electrophoresis. Extensive clinical investigations are necessary to define and validate an effective biomarker based on the protein corona that takes into account all the factors that may influence its specificity and sensitivity.

## REFERENCES

[1]M. Wrensch, Y. Minn, T. Chew, M. Bondy, and M. S. Berger, Neuro-oncology **4**(4), 278 (2002).

[2]A. Hutter, K. E. Schwetye, A. J. Bierhals, and R. C. McKinstry, Neuroimaging Clin. North Am. **13**(2), 237 (2003).

[3]M. Mehta, M. A. Vogelbaum, S. Chang, and N. Patel, Cancer, Principles and Practice of Oncology **9**, 1700 (2011); D. N. Louis, H. Ohgaki, O. D. Wiestler, W. K. Cavenee, P. C. Burger, A. Jouvet, B. W. Scheithauer, and P. Kleihues, Acta Neuropathol. **114**(2), 97 (2007).

[4]R. Stupp, J.-C. Tonn, M. Brada, G. Pentheroudakis, and ESMO Guidelines Working Group, Ann. Oncol. **21**(5), v190 (2010).

[5]J. T. Cole and N. B. Holland, Drug Delivery Transl. Res. **5**(3), 295 (2015).

[6]M. P. Monopoli, C. Åberg, A. Salvati, and K. A. Dawson, Nat. Nanotechnol. **7**(12), 779 (2012); G. Caracciolo, Nanomed: Nanotechnol., Biol. Med. **11**(3), 543 (2015).

[7]A. Bigdeli, S. Palchetti, D. Pozzi, M. R. Hormozi-Nezhad, F. B. Bombelli, G. Caracciolo, and M. Mahmoudi, ACS Nano **10**(3), 3723 (2016); E. Valsami-Jones and I. Lynch, Science **350**(6259), 388 (2015); G. Ciasca, M. Papi, M. Chiarpotto, M. Rodio, G. Campi, C. Rossi, P. De Sole, and A. Bianconi, Appl. Phys. Lett. **100**(7), 073703 (2012); G. Caracciolo, F. Cardarelli, D. Pozzi, F. Salomone, G. Maccari, G. Bardi, A. L. Capriotti, C. Cavaliere, M. Papi, and A. Laganà, ACS Appl. Mater. Interfaces **5**(24), 13171 (2013); M. Papi, M. C. Lauriola, V. Palmieri, G. Ciasca, G. Maulucci, and M. De Spirito, RSC Adv. **5**(99), 81638 (2015).

[8]M. Mahmoudi, S. N. Saeedi-Eslami, M. A. Shokrgozar, K. Azadmanesh, M. Hassanlou, H. R. Kalhor, C. Burtea, B. Rothen-Rutishauser, S. Laurent, and S. Sheibani, Nanoscale **4**(17), 5461 (2012); M. J. Hajipour, S. Laurent, A. Aghaie, F. Rezaee, and M. Mahmoudi, Biomater. Sci. **2**(9), 1210 (2014); G. Caracciolo, D. Pozzi, A. L. Capriotti, C. Cavaliere, S. Piovesana, H. Amenitsch, and A. Laganà, RSC Adv. **5**(8), 5967 (2015); M. J. Hajipour, J. Raheb, O. Akhavan, S. Arjmand, O. Mashinchian, M. Rahman, M. Abdolahad, V. Serpooshan, S. Laurent, and M. Mahmoudi, Nanoscale **7**(19), 8978 (2015); V. Mirshafiee, R. Kim, M. Mahmoudi, and M. L. Kraft, Int. J. Biochem. Cell Biol. **75**, 188 (2016); C. Corbo, R. Molinaro, A. Parodi, N. E. Toledano Furman, F. Salvatore, and E. Tasciotti, Nanomedicine **11**(1), 81 (2016); S. Palchetti, V. Colapicchioni, L. Digiacomo, G. Caracciolo, D. Pozzi, A. L. Capriotti, G. L. Barbera, and A. Laganà, Biochim. Biophys. Acta **1858**(2), 189 (2016); M. Lundqvist, J. Stigler,

[9]D. Pozzi, V. Colapicchioni, G. Caracciolo, S. Piovesana, A. L. Capriotti, S. Palchetti, S. De Grossi, A. Riccioli, H. Amenitsch, and A. Laganà, Nanoscale **6**(5), 2782 (2014).

[10]M. Lundqvist, C. Augustsson, M. Lilja, K. Lundkvist, B. Dahlbäck, S. Linse, and T. Cedervall, PLoS One **12**(4), e0175871 (2017).

[11]T. Zheng, N. Pierre-Pierre, X. Yan, Q. Huo, A. J. Almodovar, F. Valerio, I. Rivera-Ramirez, E. Griffith, D. D. Decker, and S. Chen, ACS Appl. Mater. Interfaces **7**(12), 6819 (2015).

[12]V. Colapicchioni, M. Tilio, L. Digiacomo, V. Gambini, S. Palchetti, C. Marchini, D. Pozzi, S. Occhipinti, A. Amici, and G. Caracciolo, Int. J. Biochem. Cell Biol. **75**, 180 (2016); D. Caputo, M. Papi, R. Coppola, S. Palchetti, L. Digiacomo, G. Caracciolo, and D. Pozzi, Nanoscale **9**(1), 349 (2017).

[13]J. Adler-Moore and R. T. Proffitt, J. Antimicrob. Chemother. **49**(suppl 1), 21 (2002).

[14]A. L. Barrán-Berdón, D. Pozzi, G. Caracciolo, A. L. Capriotti, G. Caruso, C. Cavaliere, A. Riccioli, S. Palchetti, and A. Laganà, Langmuir **29**(21), 6485 (2013); G. Caracciolo, D. Pozzi, A. L. Capriotti, C. Cavaliere, P. Foglia, H. Amenitsch, and A. Laganà, ibid. **27**(24), 15048 (2011); M. Mahmoudi, A. M. Abdelmonem, S. Behzadi, J. H. Clement, S. Dutz, M. R. Ejtehadi, R. Hartmann, K. Kantner, U. Linne, and P. Maffre, ACS Nano **7**(8), 6555 (2013); S. Tenzer, D. Docter, J. Kuharev, A. Musyanovych, V. Fetz, R. Hecht, F. Schlenk, D. Fischer, K. Kiouptsi, and C. Reinhardt, Nat. Nanotechnol. **8**(10), 772 (2013).

[15]J. Schindelin, I. Arganda-Carreras, E. Frise, V. Kaynig, M. Longair, T. Pietzsch, S. Preibisch, C. Rueden, S. Saalfeld, and B. Schmid, Nat. Methods **9**(7), 676 (2012).

[16]M. Papi, D. Caputo, V. Palmieri, R. Coppola, S. Palchetti, F. Bugli, C. Martini, L. Digiacomo, D. Pozzi, and G. Caracciolo, Nanoscale **9**(29), 10327 (2017); V. Palmieri, G. Lucchetti, I. Gatto, A. Maiorana, M. Marcantoni, G. Maulucci, M. Papi, R. Pola, M. De Spirito, and A. Sgambato, J. Nanopart. Res. **16**(9), 2583 (2014).

[17]G. Caracciolo, S. Palchetti, L. Digiacomo, R. Z. Chiozzi, A. L. Capriotti, H. Amenitsch, P. M. Tentori, V. Palmieri, M. Papi, F. Cardarelli, D. Pozzi, and A. Laganà, ACS Appl. Mater. Interfaces **10**, 22951–22962 (2018).

[18]M. Colafranceschi, M. Papi, A. Giuliani, G. Amiconi, and A. Colosimo, Pathophysiol. Haemostasis Thromb. **35**(6), 417 (2006); M. Papi and G. Caracciolo, Nano Today **21**, 14–17 (2018).

[19]T. Jombart, S. Devillard, and F. Balloux, BMC Genet. **11**(1), 94 (2010).

[20]K. Khan, R. Hardy, A. Haq, O. Ogunbiyi, D. Morton, and M. Chidgey, Br. J. Cancer **95**(10), 1367 (2006); E. P. Parrish, D. R. Garrod, D. L. Mattey, L. Hand, P. V. Steart, and R. O. Weller, Proc. Natl. Acad. Sci. **83**(8), 2657 (1986).

[21]H. N. Banerjee, K. Mahaffey, E. Riddick, A. Banerjee, N. Bhowmik, and M. Patra, Mol. Cell. Biochem. **367**(1–2), 59 (2012).